Published online 21 February 2007 *Nucleic Acids Research, 2007, Vol. 35, No. 5* ***1737–1749***
doi:10.1093/nar/gkm073

Interactions of Kid–Kis toxin–antitoxin complexes with the *parD* operator-promoter region of plasmid R1 are piloted by the Kis antitoxin and tuned by the stoichiometry of Kid–Kis oligomers

Maria C. Monti[1], Ana M. Hernández-Arriaga[2], Monique B. Kamphuis[3], Juan López-Villarejo[2], Albert J. R. Heck[1], Rolf Boelens[3], Ramón Díaz-Orejas[2] and Robert H. H. van den Heuvel[1,*]

[1]Bijvoet Center for Biomolecular Research and Utrecht Institute for Pharmaceutical Sciences, Department of Biomolecular Mass Spectrometry, Utrecht University, Sorbonnelaan 16, 3584 CA Utrecht, The Netherlands, [2]Centro de Investigaciones Biológicas, Departamento de Microbiología Molecular, Ramiro de Maeztu 9, E-28040 Madrid, Spain and [3]Bijvoet Center for Biomolecular Research, Department of NMR Spectroscopy, Utrecht University, Padualaan 8, 3584 CH Utrecht, The Netherlands

Received October 17, 2006; Revised December 30, 2006; Accepted January 24, 2007

ABSTRACT

The *parD* operon of *Escherichia coli* plasmid R1 encodes a toxin–antitoxin system, which is involved in plasmid stabilization. The toxin Kid inhibits cell growth by RNA degradation and its action is neutralized by the formation of a tight complex with the antitoxin Kis. A fascinating but poorly understood aspect of the *kid–kis* system is its autoregulation at the transcriptional level. Using macromolecular (tandem) mass spectrometry and DNA binding assays, we here demonstrate that Kis pilots the interaction of the Kid–Kis complex in the *parD* regulatory region and that two discrete Kis-binding regions are present on *parD*. The data clearly show that only when the Kis concentration equals or exceeds the Kid concentration a strong cooperative effect exists between strong DNA binding and Kid_2–Kis_2–Kid_2–Kis_2 complex formation. We propose a model in which transcriptional repression of the *parD* operon is tuned by the relative molar ratio of the antitoxin and toxin proteins in solution. When the concentration of the toxin exceeds that of the antitoxin tight Kid_2–Kis_2–Kid_2 complexes are formed, which only neutralize the lethal activity of Kid. Upon increasing the Kis concentration, $(Kid_2–Kis_2)_n$ complexes repress the *kid–kis* operon.

INTRODUCTION

Toxin–antitoxin systems in bacteria eliminate plasmid-free cells that emerge as a result of segregation or replication defects and they contribute to intra- and interspecies plasmid dissemination (1–3). Plasmid-encoded toxin–antitoxin systems and their chromosomal homologues are widespread in bacteria. Chromosomal toxin–antitoxin systems have been proposed to induce reversible cell cycle arrest or plasmid stabilization in response to nutritional and/or environmental stress. Toxin–antitoxin cassettes have a characteristic organization in which the gene encoding the toxin follows the gene encoding the antitoxin. The two loci have often a common autoregulatory mechanism exerted by both components. The toxin gene encodes a stable protein, whereas the antitoxin is either a non-translated, antisense RNA species (type I) or a labile protein (type II).

The majority of the plasmid and chromosome-encoded toxin–antitoxin loci is of the type II module (2). The toxin and antitoxin form a tight complex so that no free toxin is present in the cell. When a plasmid-free daughter cell is produced, owing to a defect in plasmid replication or maintenance, the newborn cell will still inherit the

*To whom correspondence should be addressed. Tel: +31 302536797; Fax: +31 302518219; Email: r.h.h.vandenheuvel@chem.uu.nl or robert.vandenheuvel@organon.com
The authors wish it to be known that, in their opinion, the first two authors should be regarded as joint First Authors
Present address:
Robert H. H. van den Heuvel, Organon, P. O. Box 20, 5340 BH Oss, The Netherlands

toxin–antitoxin protein complex. However, the antitoxin component is degraded easily by host proteases and is not refreshed because of the absence of the plasmid encoding for the toxin–antitoxin system. The toxin will then act on an essential host target to cause growth impairment or cell death of the plasmid-free cell. In spite of the many studies on type II toxin–antitoxin systems, only two intracellular targets have been identified. CcdB and ParE are known to act on DNA gyrase (4,5), RelE mediates cleavage of mRNA in a ribosome-dependent manner, thereby affecting the level of protein synthesis (6) and MazF, Kid and YoeB proteins have been found to show ribosome-independent RNase activity (7–10).

Toxin–antitoxin systems that have been studied so far are autoregulated at the level of transcription by binding of the antitoxin to the operator-promoter region of the operon, however, the underlying molecular mechanism of this autoregulation is poorly understood. Several toxin–antitoxin pairs repress the transcription of their toxin–antitoxin operons, such as *mazEF*, *relBE*, *kid–kis*, *ccd*, *higAB* and *doc-phd*, indicating that an autoregulation process involving one or both proteins may be a common feature for these operons (11–15). In most of the cases, the antitoxin is directly responsible for the repression, but the toxin can also assist by increasing the affinity of the regulatory complex.

In *Escherichia coli*, the *parD* operon of plasmid R1 encodes the toxin Kid (Killing determinant) and the antitoxin Kis (Killing suppressor) (16). Kid is a ribonuclease, which cleaves RNA preferentially at the 5′ side of the adenosine residue in the nucleotide sequence 5′-UA(A/C)-3′ of single-stranded regions, although cleavage in double-stranded regions and at the 3′ side of the adenosine has been observed as well (17,18). Kis prevents the inhibition of *E. coli* cell growth caused by Kid. Kis autoregulates *parD* transcription to a limited extent and this activity can be allocated to the N-terminal region of the protein (19). The coordinate action of the Kid–Kis complexes has been shown to efficiently repress *parD* transcription (11,18,20). In addition, synthesis of the Kid toxin is coupled to the synthesis of the Kis antitoxin and the intracellular levels of these proteins are also controlled by limited degradation of a polycistronic messenger (21). These regulatory mechanisms avoid the synthesis of the toxic component in case its antitoxin has not been translated previously and ensures a balanced production of the antitoxin relative to the toxin (22).

For *mazEF* and *ccd* addiction complexes it has been shown that the toxin and antitoxin can form various assemblies with different stoichiometries (23–25). Dao-Thi *et al*. (23) have proposed a model in which $(CcdA_2\text{-}CcdB_2)_n$ complexes interact with multiple DNA-binding sites and spiral around the 120-bp promoter region. Kis and Kid also form various complexes. The Kid_2–Kis_2–Kid_2 heterohexamer is the most abundant species when Kid is in excess of Kis, whereas at higher concentrations of Kis, various complexes are present ranging from Kid_2–Kis_2 tetramer up to heterodecamers, however, the function of these complexes and especially the interactions with operator-promoter DNA has not been elucidated (M.B. Kamphuis *et al*., submitted for publication).

In this study, we aimed to unravel the mechanism of autoregulation at the transcriptional level of the type II toxin–antitoxin system *kid–kis* by analyzing the Kid–Kis complexes formed at the *parD* operon. We focused on the dynamic changes of the stoichiometry of Kid–Kis oligomers induced by binding of the *parD* operon and on their different binding affinity by using electrophoretic mobility shift assays, hydroxyl radical footprinting and macromolecular mass spectrometry. Mass spectrometry is a relatively new player in the field of structural biology of non-covalent protein–nucleic acid complexes, which allows for the analysis of multiple species in a single experiment (26,27). Moreover, in combination with gas-phase dissociation experiments, the data also provide insight in the global organization of complexes (28–30). Based on our results, we present a detailed model, which explains the transcriptional autoregulation process of the *parD* operon.

MATERIALS AND METHODS

Proteins and DNA

Kid toxin, ^{15}N-labelled Kis antitoxin and His-tagged Kis were overexpressed and purified essentially as described previously (18,31, M.B. Kamphuis *et al*., submitted for publication). The predicted masses for these proteins on the basis of the primary sequence were 12 038, 9689 and 10 885 Da, respectively.

The dsDNA fragments used for the DNA binding and footprinting assays were obtained from PCR amplification using the *Sau*3A fragment from pKN1562 as DNA template, including the *parD* operator-promoter region, cloned into the *Bam*HI site of pUC18. Oligonucleotides (1) 5′-TATGGAAGCAACCACGCT-3′, (2) 5′-TCAGCATAACTGAGCC-3′, (3) 5′-GTGCGTT AAAGCCTGGTGTGT-3′ and (4) 5′-CACACCAGGCT TTAACGCAC-3′ were synthesized. PCR was performed after 5′-end labelling of one of the oligonucleotides with [γ-^{32}P] ATP and T4 polynucleotide kinase. The size of the amplification products was 175-bp (oligonucleotides 1 and 2), 81-bp (oligonucleotides 1 and 4) and 115-bp (oligonucleotides 2 and 3). The 175-bp DNA fragment contains the operator-promoter of the *parD* operon (including region I and II) (Figure 2C), whereas the 115-bp and 81-bp DNA fragments contain only region I or II, respectively (Figure 4A and B). Each DNA fragment was analysed on a 5% polyacrylamide native gel. The end-labelled DNA fragments were eluted from the gel at 42°C for 12 h in a buffer containing sodium chloride (200 mM), Tris/hydrochloride (20 mM) and ethylenediamine tetraacetic acid (2 mM), pH 7.4. For mass spectrometry studies, we used a 30-bp *parD* DNA fragment (upper strand 5′-GGATGTTATATTTAA ATATAACTTTTATGG-3′), containing *parD* region I plus 2 bp upstream and 5 bp downstream and a 30-bp dsDNA fragment with a random sequence (upper strand 5′-AGCTGCCAGGCACCAGTGTCAGCGTCCTAT-3′).

Macromolecular mass spectrometry

All mass spectrometry studies were performed in aqueous ammonium acetate (100 mM), pH 5.8. Mixtures of Kis, Kid and 30-bp *parD* region I DNA fragment were incubated at 20°C for 5 min before analysis. The Kis concentration was fixed at 7.5 μM when Kis alone or a Kid:Kis mixture at 2:1 molar ratio was incubated with dsDNA, whereas the Kis concentration was 15 μM when a Kid:Kis mixture at 1:1 molar ratio was incubated with *parD* DNA. The Kis:*parD* DNA molar ratios ranged from 80:1 to 20:1. Borosilicate glass capillaries (Kwik-Fil, World Precision Instruments, Inc., Sarasota, FL, USA) were used on a P-97 puller (Sutter Instrument Co., Novato, CA, USA) to prepare the nanoflow electrospray capillaries with an orifice of about 5 μm. The capillaries were subsequently coated with a thin gold layer (~500 Å) by using an Edwards ScanCoat Six Pirani 501 sputter coater (Edwards High Vacuum International, Crawley, UK).

For native mass spectrometry experiments, samples were introduced into a nanoflow electrospray ionization orthogonal time-of-flight mass spectrometer (Micromass LC-T, Waters, Manchester, UK) modified for high mass operation and operating in positive ion mode. To generate intact ions *in vacuo* from protein complexes in solution, the ions were cooled by increasing the pressure in the first vacuum stages of the mass spectrometer. The pressure in the source region was adjusted to 7.0 mbar by reducing the pumping capacity of the rotatory pump by closing the speed-valve (32). In addition, nanoflow electrospray voltages were optimized for transmission of intact protein complexes and for efficient desolvation using capillary and cone voltages of 1200–1300 V and 50–60 V, respectively. All spectra were mass calibrated by using an aqueous solution of cesium iodide (5 mg/ml).

Tandem mass spectrometry is routinely used for the fragmentation of peptides, and more recently also for the gas-phase dissociation of protein complexes (29,30,33,34). In these experiments, ions of a defined m/z ratio are isolated by a (high-mass) quadrupole analyzer and subsequently dissociated by increasing the acceleration voltage in a gas-filled, usually argon or xenon, collision cell. Experimentally, it has been demonstrated that a preference is expected for the dissociation of the smallest protein and/or proteins that are at the surface of the complex. The proteins that dissociate usually take up a relatively large number of charges (35). For gas-phase dissociation experiments, samples were introduced into a Micromass Q-ToF 1 mass spectrometer (Waters, Manchester, UK) equipped with a nanoflow Z-spray source and modified for high mass-to-charge ion isolation and high mass operation (29) and operating in positive ion mode. Precursor ions of selected complex compositions were isolated in the quadrupole analyzer and accelerated into an argon-filled collision cell. Different collision energies (10–150 V) were used in combination with a gas pressure of 0.8 mbar. The voltages were optimized for transmission of intact protein complexes and for efficient desolvation using capillary and cone voltages of 1200 and 60 V, respectively. To confirm each result, at least two independent charge states were selected for each protein–*parD* DNA complex.

Mass spectrometry data analysis

The mass spectrometry data were semi-quantified to determine the relative amount of the protein complexes present in the different experiments. Data were accumulated over 2 min, averaged, smoothed and centred, thereby using the areas option in the software program MassLynx 4.0 (Waters). The total ion intensity for each complex was calculated by summing the intensity of all ions belonging to the Gaussian charge state envelope of the protein complex under analysis. The percentage of each protein complex was then calculated by using the total ion intensity of all identified protein complexes. The calculated relative abundances were based on two independent measurements.

Electrophoretic mobility shift assays

Binding of Kid and Kis proteins to 5′-end-labelled 175-bp *parD* region I/II, 81-bp *parD* region II or 115-bp *parD* region I fragment (1.4×10^6 c.p.m./mol) was determined according to a previously described method (36) with modifications. The binding reactions contained end-labelled DNA (2 nM), Tris/hydrochloride (70 mM), potassium chloride (200 mM), magnesium chloride (14 mM), sodium chloride (80 mM), ethylenediamine tetraacetic acid (40 mM), bovine serum albumin (100 μg/ml), glycerol (0.5% (v/v)) and Kid (2.4 μM) and/or Kis (0.075–9.6 μM). The assays were also performed with higher *parD* DNA concentrations (375 nM) and Kis (7.5 or 15 μM) and/or Kid (7.5 or 15 μM). The mixtures were incubated at 4°C for 60 min. Where indicated, poly [d(I-C)] (70 μM) as non-specific competitor DNA was added and incubation was continued for another 5 min at the same temperature. Free and bound *parD* DNA fragments were separated on polyacrylamide (5 or 8% (w/v)) native gels. The gels were run at 4°C in TBE buffer (Tris/hydrochloride (89 mM), boric acid (89 mM) and ethylenediamine tetraacetic acid (10 mM), pH 8.9) at 100 V for 60 min. The labelled DNA bands were visualized by autoradiography.

Hydroxyl radical footprinting

5′-End-labelled 175-bp *parD* region I/II or 115-bp *parD* region I fragment was incubated with Kid (2.4 μM) and/or Kis (4.8 μM) under the same conditions as in the electrophoretic mobility shift assays. After incubation, a solution containing iron sulphate (100 μM), ethylenediamine tetraacetic acid (200 μM), sodium ascorbate (1 mM) and hydroperoxide (0.3%) was added, and the mixture was incubated at 4°C for 5 min. The cleavage reaction was terminated by the addition of a mixture containing thiourea (8 mM) and ethylenediamine tetraacetic acid (1.7 mM). DNA–protein complexes were separated from free DNA by polyacrylamide 5% (w/v) gel electrophoresis and visualized by autoradiography. Bound DNA was eluted from gels at 42°C for 12 h, in buffer sodium chloride (200 mM), Tris/hydrochloride (20 mM) and ethylenediamine tetraacetic acid (2 mM), pH 8.0.

The DNA was precipitated with ethanol, dissolved in formamide-dye solution and analysed by polyacrylamide 8% (w/v) gel electrophoresis in the presence of urea (8 M). The cleavage products were visualized by autoradiography.

RESULTS

Antitoxin Kis, but not toxin Kid, interacts with *parD* DNA

Antitoxin Kis is known to be a weak transcriptional repressor of the *parD* operon, however, the characteristics of its interaction with the regulatory region of this operon are unknown (19). We first analysed by electrophoretic mobility shift assays, the interaction of Kis with a 175-bp DNA fragment (*parD* region I/II) containing sequences that include the operator-promoter region of the *parD* operon and further upstream sequences (Figure 1A). At Kis:*parD* region I/II molar ratios lower than 1200:1 no complex was observed between the protein and the *parD* DNA. At molar ratios of 1200:1 and 2400:1 (lanes 7 and 8) both free DNA and a mobility-shifted complex (c0) was observed, whereas at a molar ratio of 4800:1 (lane 9) no free *parD* DNA was observed. These data clearly show that Kis interacts with low affinity with the *parD* operon and the sharp transition from unbound DNA to the c0 complex points to a strong cooperative interaction of Kis onto the operator-promoter region.

The specific Kis contacts on the 175-bp parD region I/II fragment were further analysed by hydroxyl radical footprinting assays. These assays showed that Kis interacts in two imperfect inverted repeats (regions I and II) of 18 bp each and separated by 33 bp (Figure 2C). Region I contains a perfect palindromic sequence whose left half overlaps with the −10 promoter element in which protection of Kis is prominent, suggesting a direct role of these interactions in *parD* regulation.

The binding of Kid was tested under the same conditions, however, no complexes of Kid and *parD* DNA were observed, confirming that the toxin does not directly interact with the *parD* operon (Figure 1A, lane 10).

Kis–*parD* DNA interactions involve dimeric Kis subunits

We synthesized a 30-bp palindromic DNA fragment of the 175-bp *parD* region I/II, comprising region I, which we could use for nanoflow electrospray ionization mass spectrometry (Figure 2C). The 175-bp fragment is not suited for mass spectrometry studies as this large fragment retains many buffer and salt molecules, which represses the ion signal and introduces many satellite ion signals. From the mass spectra of the 30-bp *parD* region I and Kis we determined their molecular masses: 18 408.3 Da for *parD* DNA and 9687 Da and 19 373 Da for monomeric and dimeric Kis, respectively (Supplementary Table 1). The determined mass of the 30-bp *parD* DNA matches exactly with the theoretical mass, whereas the determined mass of monomeric Kis corresponds well with the mass as calculated from the primary sequence of ^{15}N-labelled Kis attached to a β-mercaptoethanol molecule (M.B. Kamphuis *et al.*, submitted for publication). Upon incubation of the 30-bp *parD* region I with a 20-fold molar excess of Kis, the mass spectrum clearly showed four charge-state distributions (Figure 3A, Supplementary Table 1). Two ion series were detected ~2000 m/z and could be assigned to monomeric and dimeric Kis and two other ion series were detected at m/z values ~4500. Mass determination of these latter two ion series revealed masses of 57 074 and 76 431 Da, which corresponds with the masses of $(Kis_2)_2$–DNA_1 and $(Kis_2)_3$–DNA_1 complexes, respectively. Upon increasing the amount of the 30-bp *parD* DNA relative to Kis (5-fold molar excess of Kis) also ions originating from free DNA and Kis_2–DNA_1 (37 801 Da) were identified (Figure 3B).

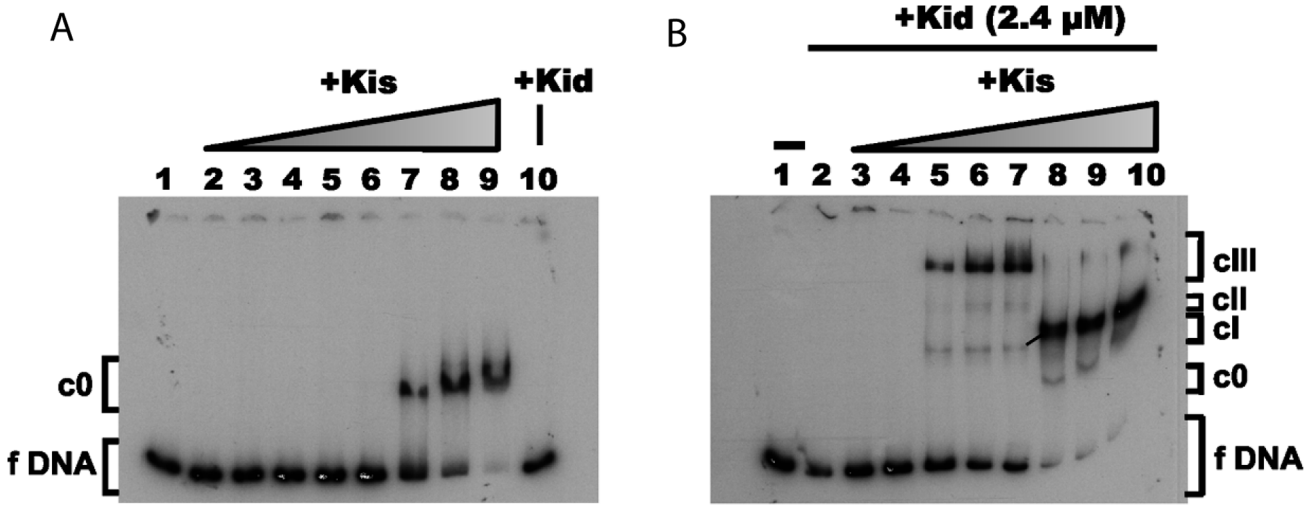

Figure 1. Effect of Kid on the interaction of Kis to *parD* DNA. Electrophoretic mobility shift assays were performed on the 5′-end-labelled 175-bp *parD* region I/II fragment (2 nM) and Kis and/or Kid. (**A**) Band-shift assays in the presence of a range of concentrations of Kis (0.075, 0.150, 0.300, 0.600, 1.2, 2.4, 4.8 and 9.6 μM) (lanes 2–9). Lane 10 presents control with only Kid (2.4 μM). (**B**) Band-shift assays over a range of Kis concentrations identical to the ones in (A) (lanes 3–10) and in the presence of a fixed concentration of Kid (2.4 μM). Lane 2 shows a control without Kid. Lane 1 presents the negative control without proteins. The specific complexes formed are indicated with c0, cI, cII and cIII.

Each protein–DNA complex involves at least one dimeric Kis unit showing that the Kis dimer is required for the specific recognition process.

Data analysis revealed that only ~15% of Kis was bound to DNA, whereas the remaining 85% was free in solution (Supplementary Table 2). This clearly demonstrates that antitoxin Kis interacts weakly with the *parD* region I. It should be noted here that ionization and transmission efficiency is protein and DNA dependent, therefore, we can only semi-quantify these data. To investigate whether the binding behaviour to the *parD* region I was indeed specific, the antitoxin Kis was added to a solution containing a 30-bp dsDNA with a random nucleotide sequence. The mass spectra did not show any protein–DNA complexes (data not shown) confirming that the recognition of the *parD* region I by Kis is highly sequence specific. As expected, incubations of Kid with the 30-bp *parD* region I did not result in the formation of binary Kid–*parD* DNA complexes.

Toxin Kid enhances antitoxin Kis binding to *parD* DNA

We performed electrophoretic mobility shift assays on complexes between Kid and Kis mixed in different

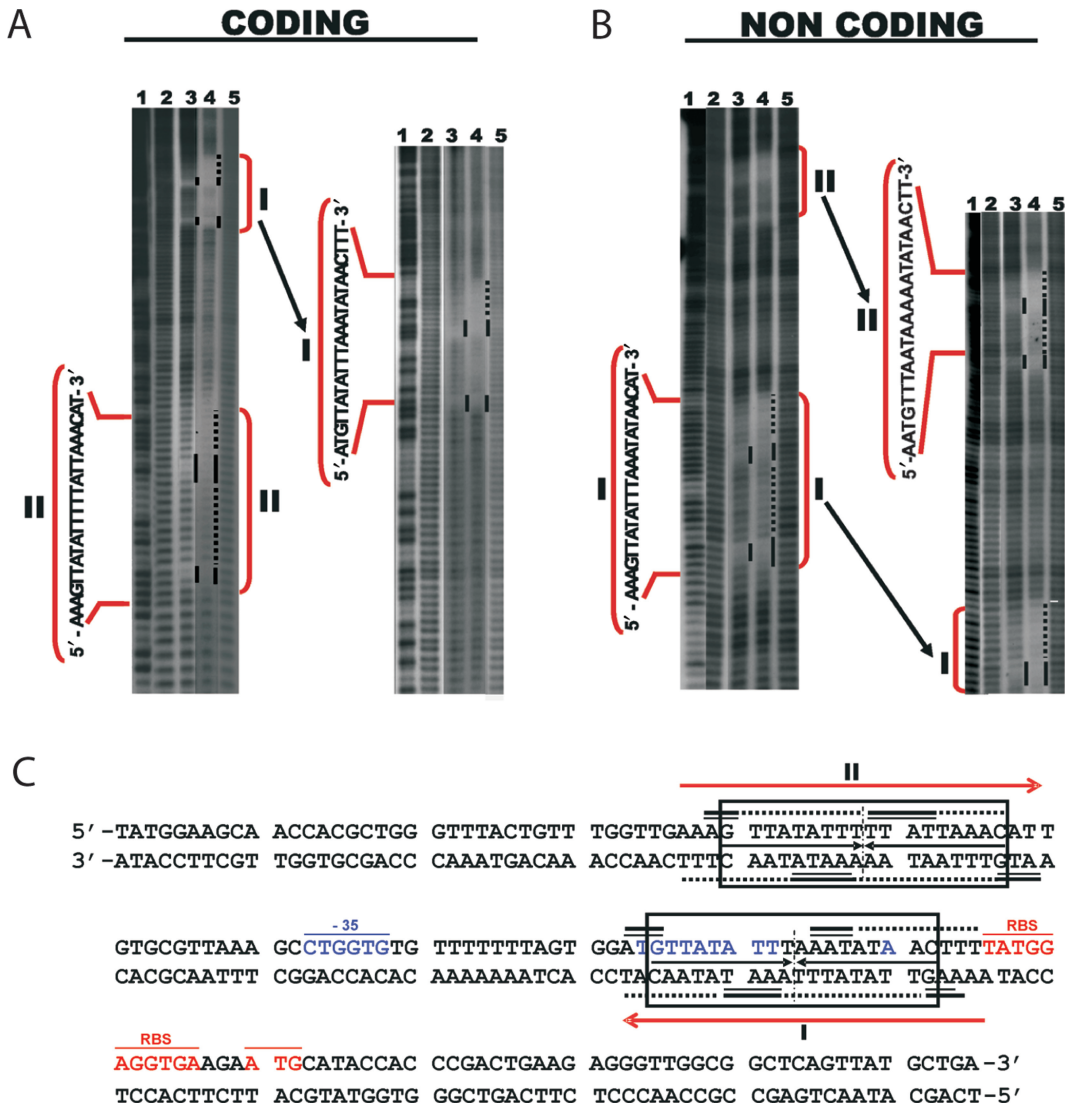

Figure 2. Kid–Kis and Kis interact at specific sites with *parD* DNA. Hydroxyl radical footprinting assays were performed on Kid–Kis mixtures (Kid–Kis ratio 1:2; Kid 2.4 and Kis 4.8 μM) and Kis (4.8 μM) alone on the 175-bp *parD* region I/II fragment. Protections in the coding (**A**) and non-coding (**B**) strands are indicated by black bars and dots. Lane 3 shows the protection pattern by Kis alone and lane 4 shows the protection pattern by the Kid–Kis complex. The sequences of the inverted repeats I and II that include the protected regions are indicated. Lanes 2 and 5 show the cleavage pattern of the DNA in the absence of any added protein. Lane 1 shows the Maxam–Gilbert AG ladder sequence. (**C**) Summary of the protected sites in *parD* region I/II by Kis and Kid–Kis complexes. The protected regions are indicated with numbers I and II. Region I contains an 18-bp perfect two-fold symmetry element (boxed) that includes the −10 motif. The site II includes an 18-bp pseudo-symmetric element that is also boxed. The dyad symmetry axis in each region is indicated with a broken line. Bases whose deoxyriboses are protected by Kis (thick bars) or Kid–Kis (thin bars) from cleavage by hydroxyl radical are indicated (underlined). DNA sequence of the −35 (underlined and labelled) and −10 elements of the promoter and the transcription initiation site are in blue. The ribosome-binding site (RBS) and translation initiation condon (Met) of *kis* are underlined and in red. The imperfect inverted repeats I and II are indicated with red arrows. The 30-bp DNA fragment used for mass spectrometry studies contains *parD* region I plus 2 bp upstream and 5 bp downstream.

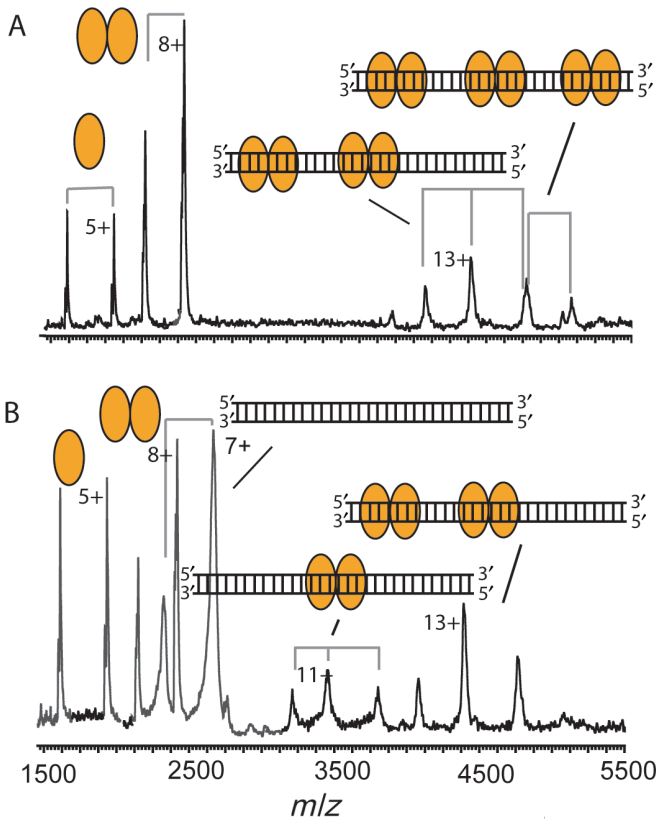

Figure 3. Dimers of Kis interact with *parD* region I. Macromolecular native mass spectrometry was performed on Kis-30-bp *parD* region I complexes in ammonium acetate (50 mM), pH 5.8. (**A**) Mass spectrum of the Kis:*parD* region I mixture at a molar ratio of 20:1 (Kis 7.5 μM). (**B**) Mass spectrum of Kis:*parD* region I mixture at a ratio of 5:1 (Kis 7.5 μM). Kis monomer and dimer are indicated with single and double orange ellipses, respectively, and the *parD* region I fragment with a double strand. Each complex is represented by an appropriate combination of ellipses and/or DNA double strand. Molecular masses and relative amounts of complexes are shown in Supplementary Tables 1 and 2, respectively.

oligomeric ratios and the 175-bp *parD* region I/II. The retardation of the *parD* DNA by Kis in the presence of a fixed concentration of Kid is shown in Figure 1B. The first mobility-shifted complexes were observed at a Kid:Kis:*parD* region I/II molar ratio of 1200:150:1 (lane 5). At this ratio, free DNA and three different mobility-shifted complexes were observed. The high intensity band was the largest complex (cIII), whereas the two additional bands (cII and cI) with lower intensity had a lower mass. The same pattern was also observed at Kid:Kis molar ratios of 4:1 and 2:1 (lanes 6 and 7).

At an equal concentration of both proteins, however, nearly no free DNA and complex cIII were detected and the intensity of complex cI was dramatically increased (lane 8). A less intense band (c0) that may correspond to DNA bound by Kis alone was also detected. The same pattern was maintained at decreased Kid:Kis molar ratios of 1:2 and 1:4 (lanes 9 and 10). These data show that when the concentration of Kis approaches that of Kid there is a dramatic shift in the complexes formed between Kid–Kis and *parD* region I/II, and the complexes with the DNA fragment become more stable. The data also show that in the presence of Kid the ternary complexes formed at higher concentrations of Kis over DNA have a lower molecular mass than the complexes formed at lower concentrations of Kis, suggesting that there are multiple binding sites for the Kid–Kis complex in the operator-promoter region of the DNA and that the ratio between the two proteins plays an important role in the formation of an efficient repressor complex. We can, however, not fully exclude that migration may also be affected by DNA bending or other conformational changes.

The Kid–Kis–*parD* DNA interactions were further analysed by DNA footprinting assays (Figure 2). At a molar ratio Kid:Kis:*parD* region I/II of 1200:2400:1, in which complexes c0 and cI were present, the protection in complex cI occurred in the same two imperfect inverted repeats (regions I and II), which were also protected by Kis alone. As Kid does not bind directly to DNA these results indicate that Kis pilots the specific interaction of this complex in the operator-promoter region. Moreover, the data show that the spacer region of 33 bp is not protected by the proteins.

parD region I interacts stronger with Kis and with Kid–Kis complexes than *parD* region II

The regions I and II were identified as the binding sites of Kis and Kid–Kis complexes in the *parD* operator-promoter region. With the aim to evaluate the binding of Kis and Kid–Kis complexes to isolated regions I and II, two different DNA fragments were produced: a 115-bp fragment comprising region I and an 81-bp fragment comprising region II (Figure 4A and B). The retardation of *parD* region I and *parD* region II by Kis is shown in Figure 4C and D. When using *parD* region I, a mobility-shifted complex (cIV) was observed at molar ratios Kis:*parD* equal or higher than 2400:1 (lanes 9 and 10), whereas, when using *parD* region II, a mobility-shifted complex (cIV) was observed at a Kis:*parD* molar ratio of 4800:1 (lane 10). These results thus show that the antitoxin Kis alone interacts specifically with both *parD* fragments, but the interaction with region I was tighter than with region II. The electrophoretic mobility shift assays were also performed with mixtures of Kid and Kis (Figure 4C and D). As in the assays with the 175-bp *parD* region I/II fragment, a fixed concentration of Kid and a variable concentration of Kis was used. For the *parD* region I fragment the first mobility-shifted complex was observed at a Kid:Kis:*parD* molar ratio of 1200:150:1 (lane 2), whereas for the *parD* region II fragment the first mobility-shifted complex was observed at a Kid:Kis:*parD* molar ratio of 1200:600:1 (lane 4). Thus, the affinity of the Kid–Kis complexes for *parD* region I is higher than for region II, which is in full agreement with the DNA binding assays using only Kis. The type of complexes formed between *parD* fragments and Kid–Kis complexes was dependent on the ratios between the two proteins. When the concentration of Kis was lower than the concentration of Kid, complex cVI was most abundant, whereas when the concentration of Kis approached the concentration of Kid, complex cV became more abundant. An additional complex (cIV) observed at an excess of Kis, may

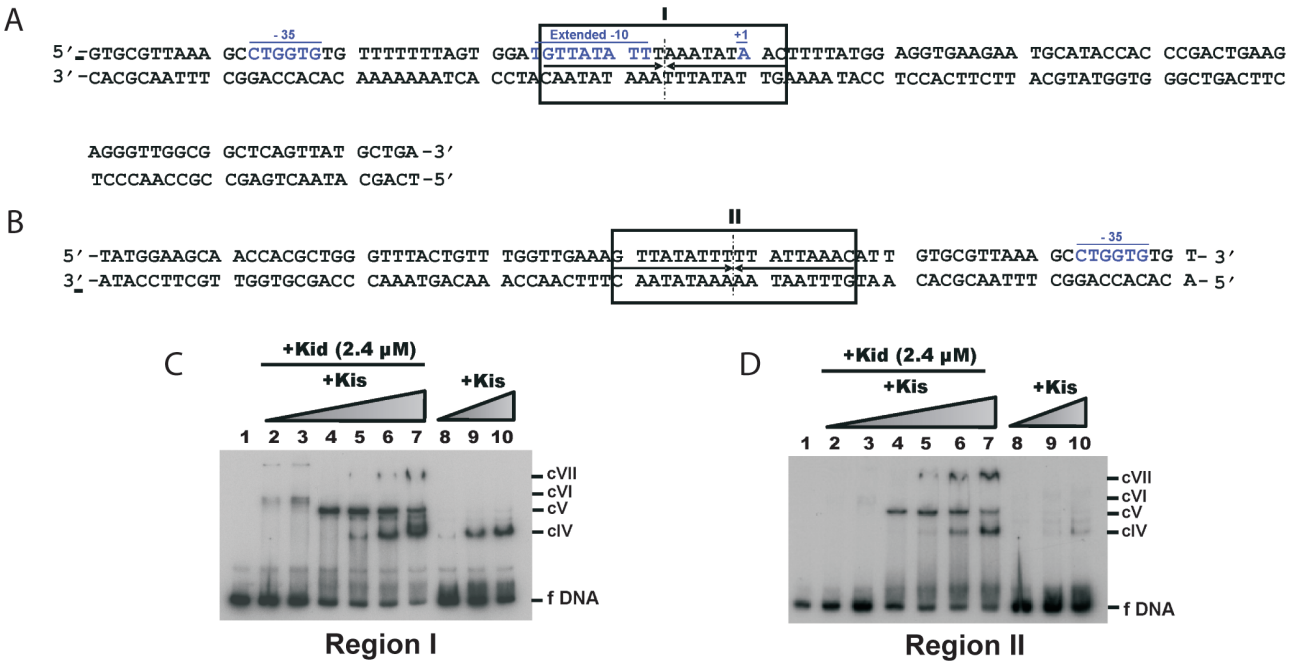

Figure 4. Kis and Kid–Kis complexes interact tighter to *parD* region I than to the *parD* region II. (**A** and **B**) Summary of the protected sites in region I and II of *parD* by Kis and Kid–Kis complexes. The 18-bp symmetric element (region I) and the 18-bp pseudo-symmetric element (region II) are boxed, and the broken lines indicate the symmetry axis. The sequence of the −35 and the extended −10 motifs and the initiation transcription (+1) are underlined and in blue. (**C** and **D**) Electrophoretic mobility shift assays were performed on the 5′-end-labelled 115-bp *parD* region I fragment (2 nM) or on the 5′-end-labelled 81-bp *parD* region II fragment (2 nM) and Kis alone (2.4, 4.8 and 9.6 μM) (lanes 8–10) or a combination of Kid (2.4 μM) and Kis (0.3, 0.6, 1.2, 2.4, 4.8 and 9.6 μM) (lanes 2–7). Lane 1 presents the negative control without proteins. The specific complexes formed are indicated with cIV, cV, cVI and cVII.

represent the binding to Kis alone, as it was also present in the incubations between Kis and *parD* DNA. A similar pattern was also observed with the *parD* region I/II fragment, although the abundance of complex c0 was very low (Figure 1). These differences between the isolated *parD* regions I and II and *parD* region I/II may suggest cooperative interactions between regions I and II.

The specific contacts between *parD* region I fragment and Kis or Kid–Kis complexes were further studied by hydroxyl footprinting assays (Supplementary Figure 1). The protection pattern clearly showed that the interactions of either Kis (cIV) or Kid–Kis complexes (cV) occur specifically on region I and involve in both cases the same backbone DNA contacts. The protection pattern observed in region I is in accordance with the footprint observed in the same operator region I in the 175-bp *parD* region I/II fragment (Figure 2). It should be noted here, however, that although the affinity with region I was higher than with region II, the protected sites observed in both regions in the 175-bp *parD* region I/II fragment had similar intensities. This again suggests cooperative interactions between regions I and II.

A molar excess of Kid results in labile $(Kid_2–Kis_2–Kid_2)_n$–*parD* DNA_1 complexes

The retardation assays showed that multiple mobility-shifted complexes can be formed between Kid, Kis and *parD* operon, but do not allow determination of the stoichiometry of the complexes. Therefore, we studied the Kid–Kis oligomers involved in interaction with the 30-bp *parD* region I by macromolecular native mass spectrometry.

Initially, Kid and Kis were mixed at a molar ratio of 2:1, yielding the Kid_2–Kis trimer (33 820 Da) and the $Kid_2–Kis_2–Kid_2$ hexamer (67 716 Da) (Supplementary Table 1; Figure 5A). Upon the addition of the *parD* region I at a molar ratio Kid:Kis:*parD* of 80:40:1 several intriguing changes were observed in the mass spectrum (Figure 5B); the trimer–hexamer equilibrium was shifted towards the hexamer and the *parD* region I interacted with the Kid–Kis complexes. The mass spectrum showed different ion series and mass determination revealed that these ion series represented free Kid dimer, Kid_2–Kis trimer, $Kid_2–Kis_2–Kid_2$ hexamer, $(Kid_2–Kis_2–Kid_2)_1$–$(DNA)_1$, (86 079 Da) $(Kid_2–Kis_2–Kid_2)_2$–$(DNA)_1$ (153 968 Da) and $(Kid_2–Kis_2–Kid_2)_3$–$(DNA)_1$ (221 957 Da) complexes. Intriguingly, in this mixture about 57% of the Kid–Kis complexes were not bound to DNA (Supplementary Table 2). These results show that at least one antitoxin Kis dimer is required for the *parD* DNA binding, also when the toxin Kid is present. Since this requirement holds only the hexamer and not the trimer, the shift of the trimer–hexamer equilibrium was induced by *parD* region I binding.

Next, we mixed the *parD* region I with Kid:Kis in a molar ratio of Kid:Kis:*parD* 20:10:1 (Figure 5C). The spectrum showed two major protein ion series corresponding to free $Kid_2–Kis_2–Kid_2$ hexamer and $Kid_2–Kis_2–Kid_2$

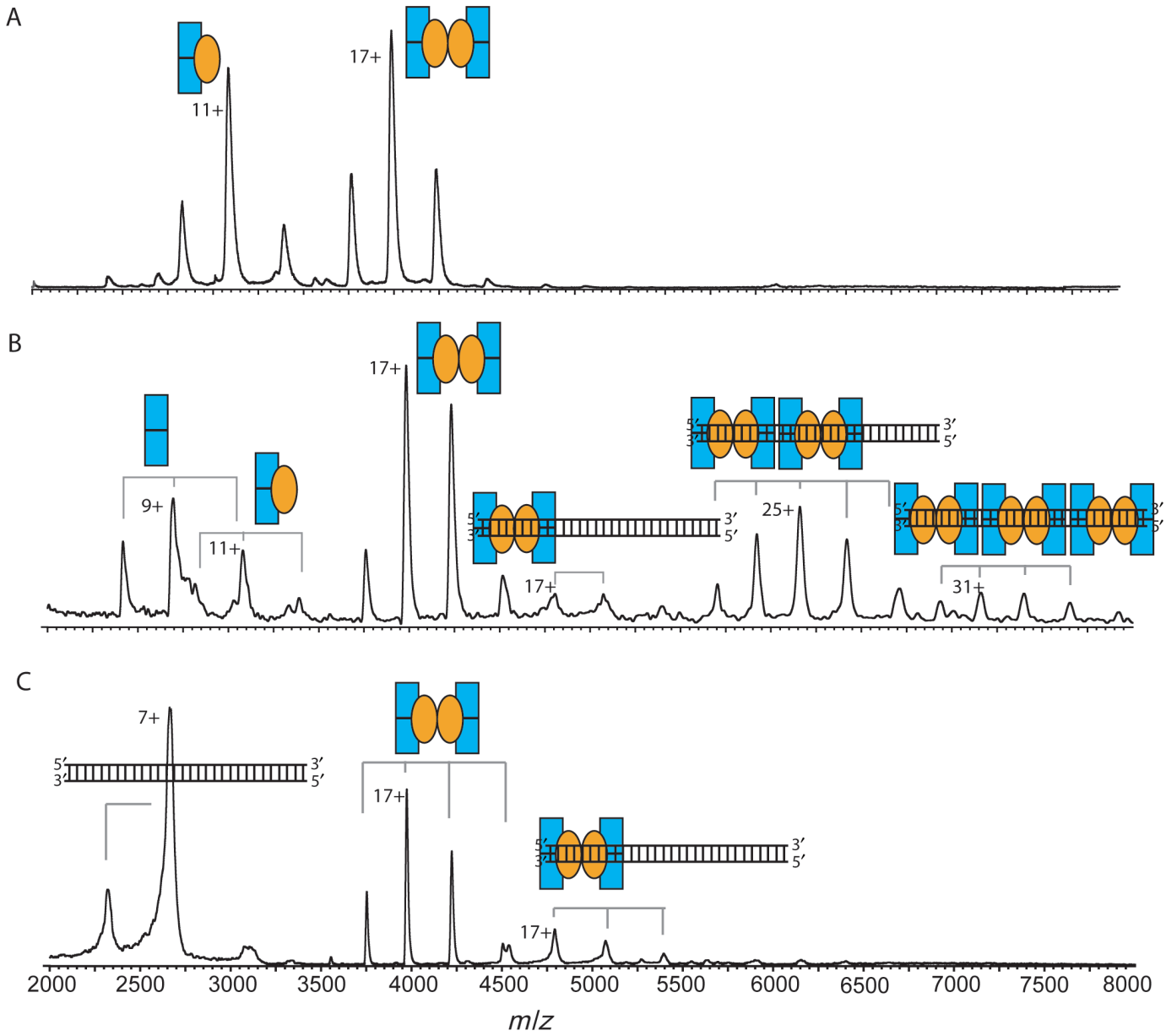

Figure 5. Kid–Kis complexes (molar ratio of 2:1) interact with *parD* region I. Macromolecular native mass spectrometry was performed on Kid–Kis and on Kid–Kis–*parD* DNA complexes in ammonium acetate (50 mM), pH 5.8. (**A**) Mass spectrum of a mixture of Kid:Kis at a molar ratio of 2:1 (Kis 7.5 μM) and (**B**) and (**C**) mass spectra of mixtures of Kid:Kis:*parD* DNA mixtures at molar ratios of 80:40:1 and 20:10:1 (Kis 7.5 μM), respectively. Kid and Kis are indicated with blue rectangles and orange ellipses, respectively, and the *parD* DNA fragment with double strand. Each complex is represented by an appropriate combination of rectangles, ellipses and/or DNA double strand. Molecular masses and relative amounts of complexes are shown in Supplementary Tables 1 and 2, respectively.

bound to *parD* DNA at a 1:1 stoichiometry (86 077 Da). These data thus clearly show that upon increasing the DNA concentration relative to Kis there is a preference for the binding of only one hexamer to the *parD* DNA. Moreover, the high amount of free Kid_2–Kis_2–Kid_2 hexamer (relative abundance of 80%) indicates a relatively low affinity between DNA and the hexameric Kid–Kis complex. This suggests that in conditions in which the Kid concentration exceeds the Kis concentration, only labile complexes are formed between *parD* DNA and Kis. This is consistent with the fact that Kid–Kis complexes formed on the 175-bp *parD* operon in excess of Kis can be easily competed by poly-(dIdC) (data not shown).

Equal concentrations of Kid and Kis induce formation of stable Kid_2–Kis_2–Kid_2–Kis_2–*parD* DNA_1 complexes

Upon mixing Kid and Kis at a 1:1 molar ratio, we observed multiple complexes: Kid_2–Kis trimer (33 841 Da), Kid_2–Kis_2 tetramer (43 450 Da), Kid_2–Kis_2–Kid_2 hexamer (67 722 Da) and Kid_2–Kis_2–Kid_2–Kis_2 octamer (87 120 Da) (Supplementary Table 1; Figure 6A).

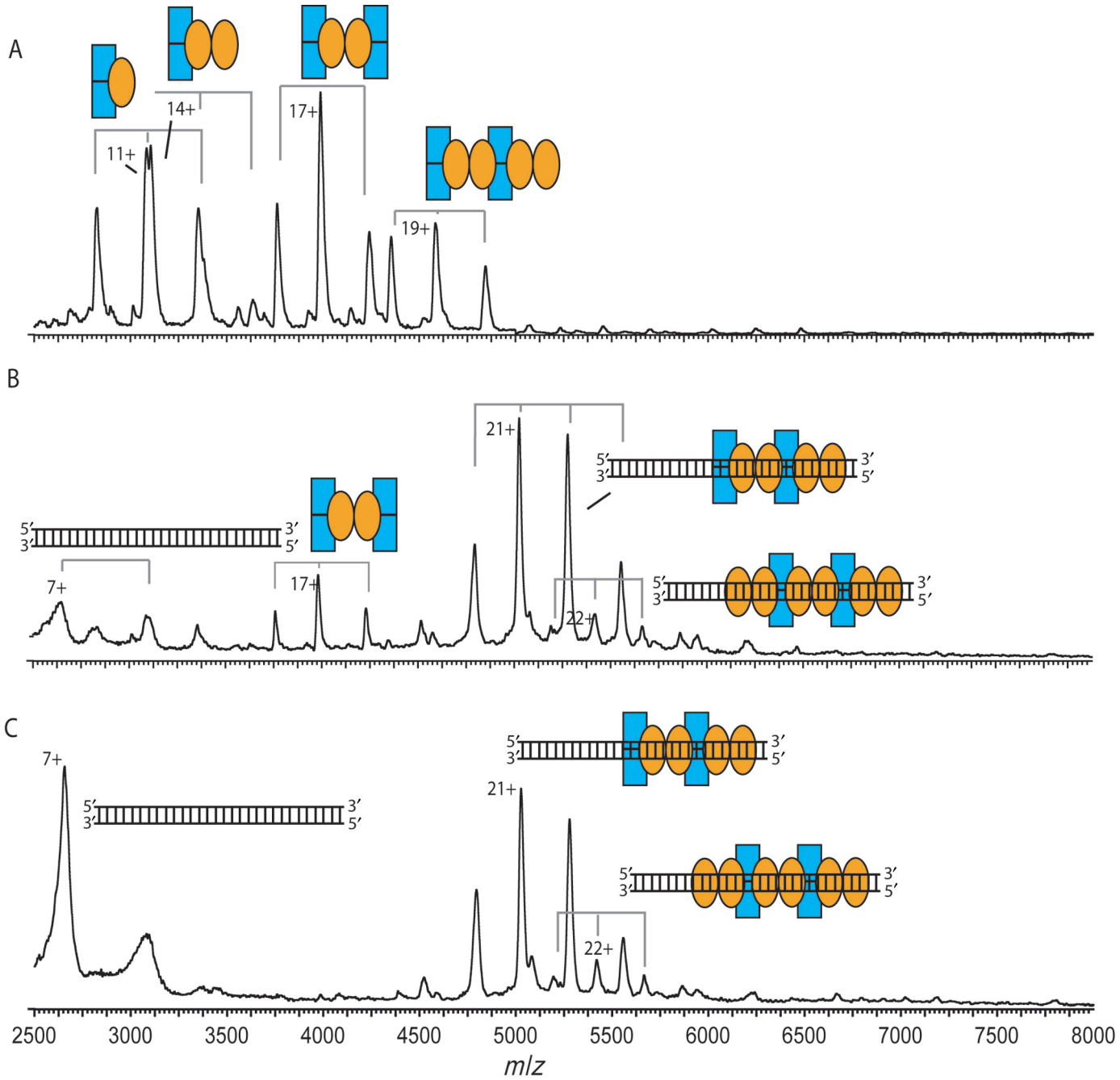

Figure 6. Kid–Kis complexes (molar ratio of 1:1) interact tightly with *parD* region I. Macromolecular native mass spectrometry was performed on Kid–Kis and on Kid–Kis–*parD* DNA complexes in ammonium acetate (50 mM), pH 5.8. (**A**) Mass spectrum of a mixture of Kid:Kis at a molar ratio of 1:1 (Kis 15 μM) and (**B**) and (**C**) mass spectra of Kid:Kis:*parD* DNA mixtures at molar ratios of 40:40:1 and 10:10:1 (Kis 15 μM), respectively. Kid and Kis are indicated with blue rectangles and orange ellipses, respectively, and the *parD* DNA fragment with double strand. Each complex is represented by an appropriate combination of rectangles, ellipses and/or DNA double strand. Molecular masses and relative amounts of complexes are shown in Supplementary Tables 1 and 2, respectively.

Upon mixing Kid–Kis mixture with the 30-bp *parD* DNA at a molar ratio of 40:40:1 and subsequent mass spectrometry analysis we observed three ion series (Figure 6B). Mass determination revealed the presence of a low amount of free Kid_2–Kis_2–Kid_2 hexamer (relative abundance of 17%) (67 675 Da) and high amounts of the DNA-bound complexes Kis_2–Kid_2–Kis_2–Kid_2–*parD* DNA_1 (76%) (105 535 Da) and Kis_2–Kid_2–Kis_2–Kid_2–Kis_2–*parD* DNA_1 (7%) (124 563 Da) complexes (Supplementary Table 2). Thus, the addition of *parD* region I to a 1:1 mixture of Kid and Kis induces a strong cooperative effect between DNA binding and Kid–Kis octamerization. This cooperative effect was even stronger when the concentration of DNA in solution

was increased 4-fold. Under these conditions the free hexamer completely disappeared and the most abundant complex became the Kis_2–Kid_2–Kis_2–Kid_2–*parD* DNA_1 complex (relative abundance of 88%) (Figure 6C). We did not observe any other changes in the mass spectrum upon increasing the concentration of *parD* DNA. These data thus clearly demonstrate that increasing the concentration of Kis relative to Kid dramatically enhances the affinity between the DNA and the Kid–Kis complexes.

Upon mixing Kid–Kis mixture with *parD* region I or II at a molar ratio of 40:40:1 or 20:20:1 and subsequent electrophoretic mobility shift analysis complexes with a similar pattern as in mass spectrometry were observed (Supplementary Figure 2). The most abundant complexes cIX and cX may represent hexameric and octameric Kid–Kis in complex with *parD* DNA, respectively. The assays also showed a faster migrating band with low abundance, which may represent the binding of hexameric Kis alone. Consistent with the mass spectrometry data *parD* region I is fully titrated when using a protein:DNA molar ratio of 20:1.

To further define the picture about the effect of the molar ratio of toxin and antitoxin on operator-promoter binding, and thus on their own expression, we added an excess of toxin or alternatively an excess of antitoxin to the Kis_2–Kid_2–Kis_2–Kid_2–*parD* DNA_1 complex. In the first experiment, a 2-fold molar excess of Kid over Kis was added to the preformed Kis_2–Kid_2–Kis_2–Kid_2–*parD* DNA_1 complex. The resulting mass spectrum showed three ion series corresponding to free DNA, Kid_2–Kis_2–Kid_2 hexamer and $(Kid_2$–Kis_2–$Kid_2)_2$–DNA_1 complex, thus revealing a partial reversion of the binding on the operator due to the excess of toxin over antitoxin. In contrast, the addition of a 2-fold molar excess of Kis over Kid to the Kis_2–Kid_2–Kis_2–Kid_2–*parD* DNA_1 complex had no effect on the equilibrium binding of the Kid_2–Kis_2–Kid_2–Kis_2 octamer to the *parD* DNA region I.

Topology of the octameric Kid–Kis–*par D* DNA complex

To further investigate the effect of *parD* DNA binding on the Kid–Kis oligomers, octameric Kid–Kis complexes free and bound to *parD* DNA were analyzed by macromolecular tandem mass spectrometry. The 20^+ ion of the free octamer (m/z 4127) was isolated by the high-mass quadrupole and subsequently accelerated in the argon-filled collision cell. Already at a low acceleration voltage (35 V) we observed dissociation of the octameric ion into highly charged monomers and moderately charged heptameric complexes (Figure 7A). At low m/z values, two charge-state envelopes were observed corresponding to Kid and Kis monomer, whereas at high m/z values, the corresponding Kis–Kid_2–Kis_2–Kid_2 and Kis_2–Kid_2–Kis_2–Kid heptamer were detected. The relative abundances of the ion peaks showed that dissociation of Kid from the octamer was somewhat favoured.

From the octameric Kid–Kis–*parD* DNA complex we selected the 21^+ (m/z 5290). At an acceleration voltage of 45 V, the Kid monomer, but not Kis monomer or *parD* region I, started to dissociate from the octamer–*parD* DNA complex (Figure 7B). Also further increasing the acceleration voltage did not result in dissociation of Kis. Thus, in comparison with free octamer, the dissociation was initiated at an increased acceleration voltage and only Kid dissociated from the DNA bound complex. This not only shows that the DNA bound complex is more stable, but also confirms the direct interaction between Kis and *parD* region I, thereby protecting the protein from dissociation. Such a phenomenon has also been observed by van Duijn *et al*. (30) for GroEL-substrate complexes, for which the substrate molecules are buried within the hydrophobic ring structure of GroEL and do not dissociate upon increasing the acceleration voltage. We did not observe any acceleration voltage-induced covalent fragmentation of *parD* DNA up to voltages of 150 V when bound to Kid–Kis octamer. In contrast, free 30-bp *parD* DNA already fragmented at an acceleration voltage of 25 V (data not shown). This data, therefore, strongly indicates that the DNA tightly interacts with the protein complex.

DISCUSSION

The *parD* operon of plasmid R1 encodes the toxin Kid and the antitoxin Kis. It has been demonstrated that *in vivo* efficient autoregulation of the *parD* operon requires the consorted action of both proteins (20). Recent *in vitro* studies have shown that Kid and Kis can form multiple complexes with different stoichiometries and oligomeric states, depending on the molar ratio between Kid and Kis (18). The Kid_2–Kis_2–Kid_2 hexamer is the most abundant species when Kid exceeds the concentration of Kis, whereas various Kid–Kis complexes are present when the concentration of Kis equals or exceeds the concentration of Kid.

Our DNA binding and mass spectrometry data presented here show that the antitoxin Kis interacts with the *parD* operon with low affinity. These data are in line with previous studies, which have shown that Kis alone is a poor repressor *in vivo* (11). The addition of toxin Kid to Kis enhances the binding affinity with *parD* DNA, however, the tightness of this interaction with *parD* DNA is determined by the molar ratio between Kid and Kis. We demonstrated that when Kid and Kis were mixed in a molar ratio of 2:1, the interaction between the resulting Kid_2–Kis_2–Kid_2 hexamer and the *parD* DNA is weak. Thus, in these conditions transcriptional repression is expected to be limited. On the contrary, when the complex mixture of Kid–Kis oligomers, obtained at an equimolar ratio of Kid and Kis, was added to the *parD* DNA a strong cooperative effect of DNA binding and Kid_2–Kis_2–Kid_2–Kis_2 octamerization was observed and the *parD* DNA interacted tightly to this octamer. We also observed that the addition of extra toxin (up to a 2-fold molar excess of Kid) to the Kid–Kis octamer–*parD* DNA complex weakened the interaction with the DNA. From these data we conclude that different molar ratios of Kid and Kis can either enhance or diminish the *parD* DNA-binding activity of Kis. Therefore, the transcriptional repression of the *parD* operon and thus the expression of Kid and Kis is critically dependent on the

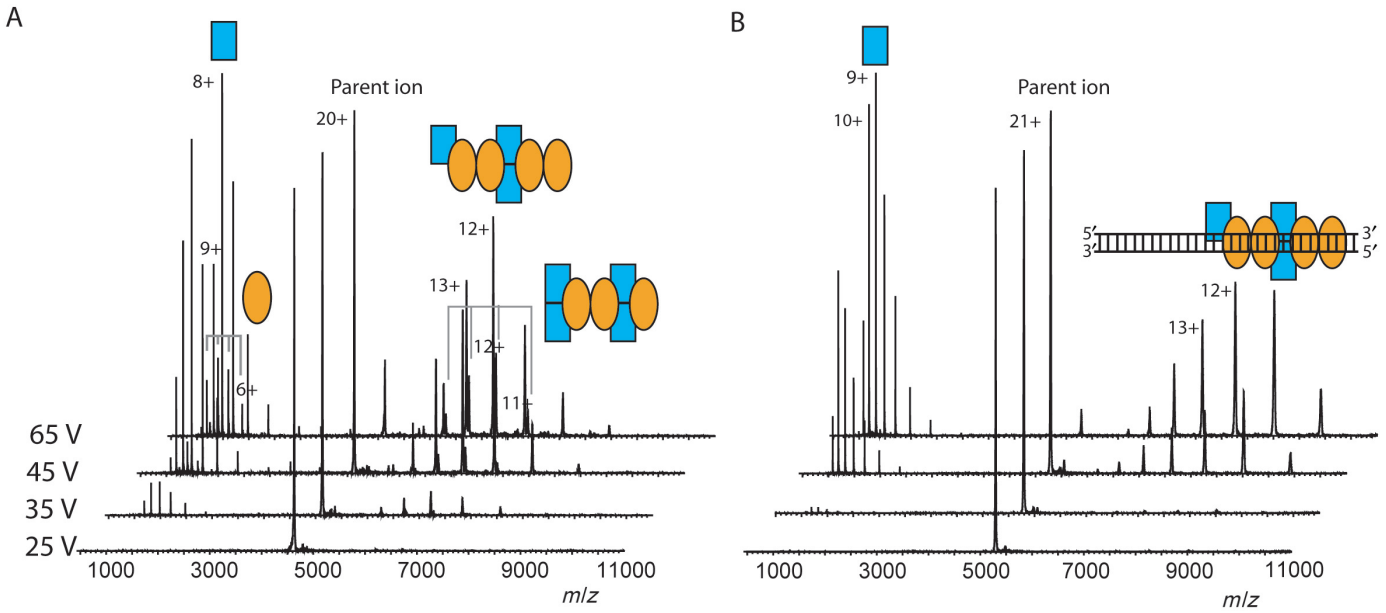

Figure 7. Macromolecular tandem mass spectrometry reveals topology of Kid–Kis–*parD* DNA region I complexes. Tandem mass spectrometry was performed on Kid–Kis and Kid–Kis–*parD* DNA in ammonium acetate (50 mM), pH 5.8. (**A**) Tandem mass spectra of Kis_2–Kid_2–Kid_2–Kis_2 after selection of the 20^+ ion and (**B**) tandem mass spectra of Kis_2–Kid_2–Kid_2–Kis_2–*parD* DNA complex after selection of the 21^+ ion. Acceleration voltages varied between 25 and 65 V. Kid and Kis are indicated with blue rectangles and orange ellipses, respectively and the *parD* DNA fragment with double strand. Each complex is represented by an appropriate combination of rectangles, ellipses and/or DNA double strand.

molar ratio of Kid and Kis. It should be noted here that the Kid–Kis octamer can interact with the two half-sites of the specific operator region (region I and II) using the two dimers of the antitoxin, whereas the Kid–Kis hexameric can interact with the two half-sites using only one dimer. This is likely to explain the more efficient binding of the octamer. Alleviation of the repression modulated by toxin and antitoxin complexes in excess of the toxin has also been reported for the *ccd* system (25,37) as well as for the *phD-doc* system (15).

Our data also show that Kis and Kid–Kis complexes interact in two imperfect inverted repeats (region I and II). Region I contains an 18-bp symmetric element and region II a pseudo-symmetric element. Moreover, by using separated fragments containing *parD* regions I or II, we found that Kis and Kid–Kis complexes interact with higher affinity to region I. The lower affinity to region II is probably due to the four non-conserved bases in this element (5′-GTTATATTT*TT*AT*TA*AAC-3′, in italic non-conserved residues). However, cooperative interactions between regions I and II potentially play an important role in the transcriptional regulation of the *parD* operon.

Are the physical parameters of the Kid–Kis complexes sufficient to form multiple interactions over the full length of the 30-bp *parD* DNA region I? Calculation of the length of the 30-bp *parD* region I and the Kid–Kis octamer, assuming a similar topology as the MazF–MazE hexamer (18,24), revealed lengths of ~100 Å for the DNA and ~150 Å for the Kid–Kis octameric complex. Although no 3D structural model is available for a Kid–Kis–DNA complex or a related toxin–antitoxin–DNA complex, it can be speculated that the octamer can fully cover the 30-bp DNA, which is in line with the DNA footprinting and tandem mass spectrometry data. Very recent nuclear magnetic resonance chemical-shift mapping data have revealed that the antitoxin CcdA alone interacts with duplex DNA comprising a 6-bp palindromic sequence (37). In here, it is also shown that a 33-bp DNA fragment, containing three potential CcdA binding sites, can bind in a cooperate manner with three CcdA dimers. The antitoxins of the *ccd* and *mazEF* systems have amino terminal regions that dimerize to form the DNA-binding region, and contain an unstructured C-terminal part, which interacts with the toxins. The toxins of these systems have also substantial structural homology (24,31), however the N-terminal domains of the CcdA and MazE antitoxin adopt different protein folds. As pointed by these authors, this surprising result confirms the proposal that gene shuffling or partner switching has been important in the evolution of the toxin–antitoxin systems (1).

Our results lead us to propose a model in which the repression of the *parD* operon is tightly regulated by the molar ratio of the toxin and the antitoxin present in the cell (Figure 8). When the level of the toxin exceeds the one of the antitoxin, stable $(Kid_2–Kis)_n$ non-covalent complexes are formed, which are able to completely neutralize Kid lethal activity (M.B. Kamphuis *et al.*, submitted for publication), but do not tightly interact with the *parD* operator-promoter region. On the contrary, when the concentration of Kis is enhanced relative to Kid, such that both proteins have similar concentrations, $(Kid_2–Kis_2)_n$ or $(Kid_2–Kis_2–Kid_2–Kis_2)_n$ oligomers are formed capable of strongly interacting with the *parD* operator-promoter region. These stoichiometric

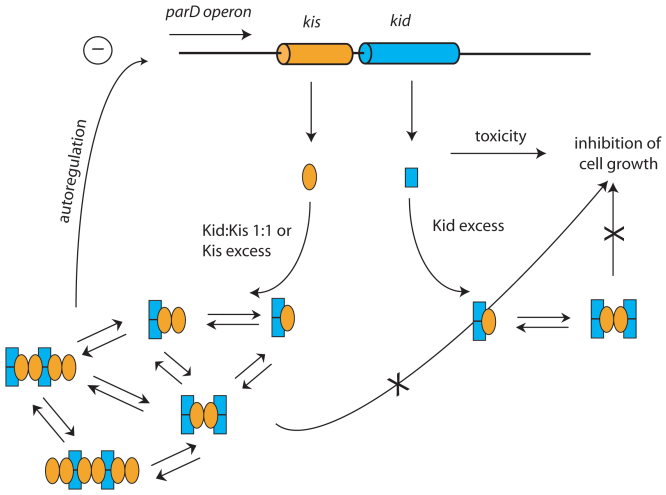

Figure 8. Schematic model of the transcription autoregulation of the *parD* operon. The *kid* gene and the Kid protein are shown in blue and the *kis* gene and the Kis protein in orange. Each protein complex is represented by an appropriate combination of blue rectangles (Kid) and orange ellipses (Kis). Free Kid inhibits cell growth. In conditions in which the concentration of Kid is higher than that of Kis Kid_2–Kis_1 and Kid_2–Kis_2–Kid_2 complexes are formed. These complexes repress ribonuclease activity of Kid, but allow efficient transcription. When the concentration of Kid is equal or lower than that of Kis, mostly 1:1 complexes are formed. These complexes do not only repress the ribonuclease activity of Kid, but also the transcription process.

complexes have a very strong capacity to interact with the specific *parD* sequences and to repress the transcription pathway. When the expression is repressed, no replacement can occur of the labile Kis antitoxin, which is prone to degradation by Lon protease. The level of the toxin will, therefore, exceed the one of the antitoxin. At this stage, the equilibrium between $(Kid_2–Kis_2)_n$ oligomers will shift towards $(Kid_2–Kis)_n$ oligomers, thereby reducing the affinity for the *parD* operon. Subsequently, the inhibition of transcription will be alleviated. The tight interaction with *parD* region I suggests that this region plays a prominent role in the regulation of *parD* repression, however, interactions in region II could be required for fine adjustment in this regulation. As mentioned above, cooperative interactions between the two regions could introduce additional complexity in this regulation. The neutralization of the negative charges of the antitoxin by the toxin may stabilize interaction of the repressor complexes with the DNA. How this particular configuration contributes to the efficient binding of the repressor complex and thus to the fine-tuning of the promoter activity remains to be established.

Similar mechanisms of transcription autoregulation have been proposed for the *ccd* and the *mazEF* addiction systems (23–25,37). Electrophoretic mobility shift assays have shown that multimers of $CcdA_2CcdB_2$ have multiple DNA-binding sites and spirals around the promoter region (25). It has also been proposed that when CcdB is present in a molar excess over CcdA, binding of a $CcdB_2$ dimer to a ($CcdB_2$-$CcdA_2$) – DNA complex causes steric hindrance and, therefore, loosens the interaction of the protein complex with DNA. This will alleviate the inhibition of transcription (37). On the other hand, for the *parD* system, the binding of Kis or Kid–Kis complexes to the *parD* operator-promoter region occurs only in two discrete regions (I and II) spaced by 33 bp; the distribution of the specific contacts that Kis and Kid–Kis complexes make on each of the DNA regions are spaced 11–13 bp, indicating that the proteins bind on the same face of the DNA. It should be noted here that CcdB and Kid have different activities: CcdB acts as a toxin and inhibitor for DNA gyrase, an essential enzyme that catalyses negative supercoiling of DNA (4), whereas Kid functions as a ribosome-independent RNase (10,18).

Although no stoichiometric complexes of MazF–MazE on the DNA have been identified, it has been postulated that MazE mediates assembly of heterocomplexes on DNA. The resulting higher order complexes would then form stoichiometric MazF–MazE complexes. In the *mazEF* system, the promoter region contains three antitoxin-binding regions (11–12-bp long) that can form an 'alternating palindrome'. It has been proposed that MazE antitoxin binds to these sites and that two MazF dimers can bridge the MazE dimers in a highly cooperative interaction (38). The situation in the *kid–kis* system is different in that the promoter region contains two binding regions, I and II, of 18-bp.

SUPPLEMENTARY DATA

Supplementary Data is available at NAR Online.

ACKNOWLEDGEMENTS

M.C.M. was supported by a Short Term FEBS Fellowship and R.H.H.vdH. by a VENI fellowship (700.54.402) from the Netherlands Organization for Scientific Research (NWO). R.D.O. was supported by Project BFU2005-03911 from the Spanish Ministry of Education and Science (MEC) and by Project PIF 200420F0332 (CSIC) and M.B.K. by the Centre for Biomedical Genetics. We thank the Netherlands Proteomics Centre for financial support. Funding to pay the Open Access publication charge was provided by Netherlands Proteomics Centre.

Conflict of interest statement. None declared.

REFERENCES

1. Anantharaman,V. and Aravind,L. (2003) New connections in the prokaryotic toxin-antitoxin network: relationship with the eukaryotic nonsense-mediated RNA decay system. *Genome Biol.*, **4**, 81.
2. Hayes,F. (2003) Toxins-antitoxins: plasmid maintenance, programmed cell death, and cell cycle arrest. *Science*, **301**, 1496–1499.
3. Gerdes,K., Christensen,S.K. and Lobner-Olesen,A. (2005) Prokaryotic toxin-antitoxin stress response loci. *Nat. Rev. Microbiol.*, **3**, 371–382.
4. Bernard,P. and Couturier,M. (1992) Cell killing by the F-plasmid Ccdb protein involves poisoning of DNA-topoisomerase-Ii complexes. *J. Mol. Biol.*, **226**, 735–745.
5. Jiang,Y., Pogliano,J., Helinski,D.R. and Konieczny,I. (2002) ParE toxin encoded by the broad-host-range plasmid RK2 is an inhibitor of Escherichia coli gyrase. *Mol. Microbiol.*, **44**, 971–979.
6. Pedersen,K., Zavialov,A.V., Pavlov,M.Y., Elf,J., Gerdes,K. and Ehrenberg,M. (2003) The bacterial toxin RelE displays

codon-specific cleavage of mRNAs in the ribosomal A site. *Cell*, **112**, 131–140.
7. Kamada,K. and Hanaoka,F. (2005) Conformational change in the catalytic site of the ribonuclease YoeB toxin by YefM antitoxin. *Mol. Cell*, **19**, 497–509.
8. Zhang,Y.L., Zhang,J.J., Hoeflich,K.P., Ikura,M., Qing,G.L. and Inouye,M. (2003) MazF cleaves cellular mRNAs specifically at ACA to block protein synthesis in Escherichia coli. *Mol. Cell*, **12**, 913–923.
9. Munoz-Gomez,A.J., Santos-Sierra,S., Berzal-Herranz,A., Lemonnier,M. and Diaz-Orejas,R. (2004) Insights into the specificity of RNA cleavage by the Escherichia coli MazF toxin. *FEBS Lett.*, **567**, 316–320.
10. Munoz-Gomez,A.J., Lemonnier,M., Santos-Sierra,S., Berzal-Herranz,A. and Diaz-Orejas,R. (2005) RNase/anti-RNase activities of the bacterial parD toxin-antitoxin system. *J. Bacteriol.*, **187**, 3151–3157.
11. Ruiz-Echevarria,M.J., Berzal-Herranz,A., Gerdes,K. and Diaz-Orejas,R. (1991) The kis and kid genes of the parD maintenance system of plasmid R1 form an operon that is autoregulated at the level of transcription by the co-ordinated action of the Kis and Kid proteins. *Mol. Microbiol.*, **5**, 2685–2693.
12. de Feyter,R., Wallace,C. and Lane,D. (1989) Autoregulation of the ccd operon in the F plasmid. *Mol. Gen. Genet.*, **218**, 481–486.
13. Gronlund,H. and Gerdes,K. (1999) Toxin-antitoxin systems homologous with relBE of Escherichia coli plasmid P307 are ubiquitous in prokaryotes. *J. Mol. Biol.*, **285**, 1401–1415.
14. Tam,J.E. and Kline,B.C. (1989) Control of the Ccd operon in plasmid-F. *J. Bacteriol.*, **171**, 2353–2360.
15. Magnuson,R. and Yarmolinsky,M.B. (1998) Corepression of the P1 addiction operon by Phd and Doc. *J. Bacteriol.*, **180**, 6342–6351.
16. Bravo,A., Ortega,S., de Torrontegui,G. and Diaz,R. (1988) Killing of Escherichia coli cells modulated by components of the stability system ParD of plasmid R1. *Mol. Gen. Genet.*, **215**, 146–151.
17. Zhang,J., Zhang,Y., Zhu,L., Suzuki,M. and Inouye,M. (2004) Interference of mRNA function by sequence-specific endoribonuclease PemK. *J. Biol. Chem.*, **279**, 20678–20684.
18. Kamphuis,M.B., Bonvin,A.M., Monti,M.C., Lemonnier,M., Munoz-Gomez,A., van den Heuvel,R.H., Diaz-Orejas,R. and Boelens,R. (2005) Model for RNA binding and the catalytic site of the RNase kid of the bacterial parD toxin-antitoxin system. *J. Mol. Biol.*, **357**, 115–126.
19. Santos-Sierra,S., Pardo-Abarrio,C., Giraldo,R. and Diaz-Orejas,R. (2002) Genetic identification of two functional regions in the antitoxin of the parD killer system of plasmid R1. *Fems Microbiol. Lett.*, **206**, 115–119.
20. Lemonnier,M., Santos-Sierra,S., Pardo-Abarrio,C. and Diaz-Orejas,R. (2004) Identification of residues of the kid toxin involved in autoregulation of the parD system. *J. Bacteriol.*, **186**, 240–243.
21. Ruiz-Echevarria,M.J., de la Cueva,G. and Diaz-Orejas,R. (1995) Translational coupling and limited degradation of a polycistronic messenger modulate differential gene expression in the parD stability system of plasmid R1. *Mol. Gen. Genet.*, **248**, 599–609.
22. de la Cueva-Mendez,G., Mills,A.D., Clay-Farrace,L., Diaz-Orejas,R. and Laskey,R.A. (2003) Regulatable killing of eukaryotic cells by the prokaryotic proteins Kid and Kis. *EMBO J.*, **22**, 246–251.
23. Dao-Thi,M.H., Charlier,D., Loris,R., Maes,D., Messens,J., Wyns,L. and Backmann,J. (2002) Intricate interactions within the ccd plasmid addiction system. *J. Biol. Chem.*, **277**, 3733–3742.
24. Kamada,K., Hanaoka,F. and Burley,S.K. (2003) Crystal structure of the MazE/MazF complex: Molecular bases of antidote-toxin recognition. *Mol. Cell*, **11**, 875–884.
25. Afif,H., Allali,N., Couturier,M. and Van Melderen,L. (2001) The ratio between CcdA and CcdB modulates the transcriptional repression of the ccd poison-antidote system. *Mol. Microbiol.*, **41**, 73–82.
26. Hanson,C.L. and Robinson,C.V. (2004) Protein-nucleic acid interactions and the expanding role of mass spectrometry. *J. Biol. Chem.*, **279**, 24907–24910.
27. van den Heuvel,R.H.H., Gato,S., Versluis,C., Gerbaux,P., Kleanthous,C. and Heck,A.J.R. (2005) Real-time monitoring of enzymatic DNA hydrolysis by electrospray ionization mass spectrometry. *Nucleic Acids Res.*, **33**, 96.
28. Sharon,M., Taverner,T., Ambroggio,X.I., Deshaies,R.J. and Robinson,C.V. (2006) Structural organization of the 19S proteasome Lid: insights from MS of intact complexes. *PLoS Biol.*, **4**, e267.
29. van den Heuvel,R.H.H., van Duijn,E., Mazon,H., Synowsky,S.A., Lorenzen,K., Versluis,C., Brouns,S.J.J., Langridge,D., van der Oost,J. *et al.* (2006) Improving the performance of a quadrupole time-of-flight mass spectrometer for macromolecular mass spectrometry. *Anal. Chem.*, **78**, 7473–7483.
30. van Duijn,E., Simmons,D.A., van den Heuvel,R.H.H., Bakkes,P.J., van Heerikhuizen,H., Heeren,R.M.A., Robinson,C.V., van der Vies,S.M. and Heck,A.J.R. (2006) Tandem mass spectrometry of intact GroEL-substrate complexes reveals substrate-specific conformational changes in the trans ring. *J. Am. Chem. Soc.*, **128**, 4694–4702.
31. Hargreaves,D., Santos-Sierra,S., Giraldo,R., Sabariegos-Jareno,R., de la Cueva-Mendez,G., Boelens,R., Diaz-Orejas,R. and Rafferty,J.B. (2002) Structural and functional analysis of the Kid toxin protein from E-coli plasmid R1. *Structure*, **10**, 1425–1433.
32. Tahallah,N., Pinkse,M., Maier,C.S. and Heck,A.J. (2001) The effect of the source pressure on the abundance of ions of noncovalent protein assemblies in an electrospray ionization orthogonal time-of-flight instrument. *Rapid Commun. Mass Spectrom.*, **15**, 596–601.
33. Sobott,F., Hernandez,H., McCammon,M.G., Tito,M.A. and Robinson,C.V. (2002) A tandem mass spectrometer for improved transmission and analysis of large macromolecular assemblies. *Anal. Chem.*, **74**, 1402–1407.
34. Videler,H., Ilag,L.L., McKay,A.R.C., Hanson,C.L. and Robinson,C.V. (2005) Mass spectrometry of intact ribosomes. *FEBS Lett.*, **579**, 943–947.
35. Benesch,J.L.P., Aquilina,J.A., Ruotolo,B.T., Sobott,F. and Robinson,C.V. (2006) Tandem mass spectrometry reveals the quaternary organization of macromolecular assemblies. *Chem. Biol.*, **13**, 597–605.
36. Garner,M.M. (1981) A gel electrophoresis method for quantifying the binding of proteins to specific DNA regions - application to components of the Escherichia coli operon regulatory system. *Nucleic Acids Res.*, **9**, 3047–3060.
37. Madl,T., van Melderen,L., Mine,N., Responsdek,M., Oberer,M., Keller,W., Khatai,L. and Zangger,K. (2006) Structural basis for nucleic acid and toxin recognition of the bacterial antitoxin CcdA. *J. Mol. Biol.*, **364**, 170–185.
38. Buts,L., Lah,J., Dao-Thi,M.H., Wyns,L. and Loris,R. (2005) Toxin-antitoxin modules as bacterial metabolic stress managers. *Trends Biochem. Sci.*, **30**, 672–679.